2012

Interface fracture of hybrid joint of glass-/steel-fiber composite

Boseman, M. F.

Emerald Group Publishing Limited

Engineering Computations International Journal for Computer-Aided Engineering and Software,

The current issue and full text archive of this journal is available at
www.emeraldinsight.com/0264-4401.htm

Received 16 June 2009
Revised 15 September 2010,
16 September 2010
Accepted 22 September 2010

Interface fracture of hybrid joint of glass-/steel-fiber composite

M.F. Boseman and Y.W. Kwon
Mechanical and Astronautical Engineering Department, Naval Postgraduate School, Monterey, California, USA, and
D.C. Loup and E.A. Rasmussen
Structures and Composite Division, Naval Surface Warfare Center, Bethesda, Maryland, USA

Abstract

Purpose – In order to connect a fiberglass composite structure to a steel structure, a hybrid composite made of glass and steel fibers has been studied. The hybrid composite has one end section with all glass fibers and the opposite end section with all steel fibers. As a result, it contains a transition section in the middle of the hybrid composite changing from glass fibers to steel fibers. The purpose of this paper is to examine interface strength at the glass to steel fiber transition section, in order to evaluate the effectiveness of the hybrid composite as a joining technique between a polymer composite structure and a metallic structure.

Design/methodology/approach – The present micromechanical study considers two types of glass to steel fiber joints: butt and overlap joints. For the butt joint, the end shape of the steel fiber is also modified to determine its effect on interface strength. The interface strength is predicted numerically based on the virtual crack closure technique to determine which joint is the strongest under various loading conditions such as tension, shear and bending. Numerical models include resin layers discretely. A virtual crack is considered inside the resin, at the resin/glass-layer interface, and at the resin/steel-layer interface. The crack is located at the critical regions of the joints.

Findings – Overall, the butt joint is stronger than the overlap joint regardless of loading types and directions. Furthermore, modification of an end shape of the middle fiber layers in the butt joint shifts the critical failure location.

Originality/value – The paper describes one of a few studies which investigated the interface strength of the hybrid joint made of fiberglass and steel-fiber composites. This joint is important to connect a polymeric composite structure to a metallic structure without using conventional mechanical joints.

Keywords Composite materials, Joining materials, Joining processes, Steels, Steel fiber, Butt joint, Overlap joint, Virtual crack closure, Hybrid

Paper type Research paper

1. Introduction

Composite materials have been used increasingly in structural applications such as aircraft, ships, automobiles, etc. because they provide unique advantages over their metallic counterparts. However, they also present complex and challenging problems to analysts and designers. Therefore, even though some structures are made of composite materials only, there are still many engineering structures which use both composite and metallic materials together. That is, a part of an overall structure is fabricated using composites while another part is made of metals. In that case, the connection between the composite and metal parts is essential and may be the critical cause for structural failure. Common joining techniques of composite and metal structures have been bolted joints (Caccese *et al.*, 2007, 2004) or bonded joints (Sihn *et al.*, 2003; Loftus *et al.*, 2002;

Engineering Computations: International Journal for Computer-Aided Engineering and Software
Vol. 29 No. 5, 2012
pp. 504-527

0264-4401
DOI 10.1108/02644401211235861

Cheuk *et al.*, 2002; Ishii *et al.*, 1998). However, bolted joints introduce stress concentration and they are labor intensive, and bonded joints have some difficulty with regard to quality control. As a result, another technique has been proposed using a hybrid composite.

A hybrid composite consists of two different fiber materials co-cured together, which are the same as those used in the structural parts to be connected. In other words, if a structure has a steel section and a glass fiber composite section to be joined, the hybrid composite is constructed of both glass and steel fibers. In particular, the hybrid laminated composite is fabricated such that one end has all glass fibers and the other end has all steel fibers with a transition in the middle. This way, the former end can be connected to the composite part of the structure while the latter end can be joined to the steel part. For example, two composite parts can be connected using the scarf joint technique (Lubkin, 1957; Hart-Smith, 1973; Erdogan and Ratwani, 1971; Baker *et al.*, 1999; Pipes *et al.*, 1982; Gunnion and Herszberg, 2006; Ganesh and Choo, 2002; Kwon *et al.*, 2008a) and two steel parts can be welded.

The strength of scarf joints as well as an improvement of their joint strength using carbon nanotubes (Kwon *et al.*, 2008b; Faulkner and Kwon, 2011; Faulkner *et al.*, 2009) has been studied. The welding technique is a well-known joining technique for metals. However, the interface joint strength of a hybrid composite made of metal and non-metal fibers, such as glass and steel fibers, is not well understood. Some previous studies investigated metal-fiber/metal-matrix composites (McGuire and Harris, 1974; Harris *et al.*, 1976). Others investigated the interface between metals and polymers (Hummelgen *et al.*, 1996; Yu *et al.*, 2002; Siau *et al.*, 2005). Only a few studies examined the interface stress and fracture toughness between glass-fiber and steel-fiber layers experimentally (Crane *et al.*, 2005; Kwon *et al.*, 2011).

Therefore, the present study examines the energy release rates of some potential cracks around the junction of two distinct fibers, such as glass and steel fibers, in order to evaluate and understand the effectiveness of the hybrid composite joint technique. Both butt and overlap joint configurations of glass and steel fibers are considered. The study is conducted numerically. The virtual crack closure (VCC) technique is used to compute energy release rates of modes I and II at critical interface locations around the junctions of glass and steel fibers under different loadings like tension, shear and bending.

The subsequent section describes the finite element modeling of a micromechanical study of interface fracture strength of glass and steel-fiber layers under different joint configurations as well as different loadings. In this section, the VCC technique adopted in the study is also explained. The next section presents the results along with explanations for three different loadings. Finally, conclusions are provided at the end.

2. Description of analysis models

In constructing a co-cured hybrid composite laminate using E-glass and steel fibers, various joint configurations may be considered with necessary load transfer from one fiber material to the other. Among them, a symmetric step/butted joint and an asymmetric step/overlap joint are commonly used in manufacturing, as shown in Figure 1. There are two critical locations of connection from E-glass- to metal-fiber layers (called metal-wire from now on), as shown in Figure 1. As a result, the present micromechanical study investigates these joining sections for their interface strength using two-dimensional plane strain models. The geometric data of the modeled

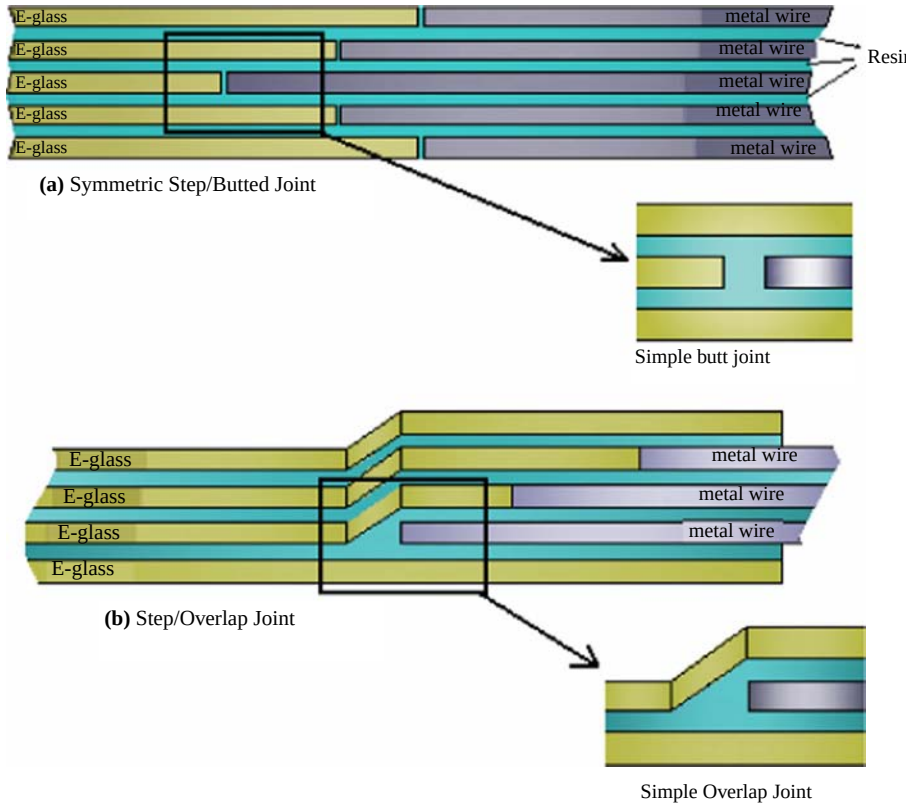

Figure 1.
Step/butted joint and step overlap joint

sections is provided in Figure 2. For the butt joint, the distance d is assumed to be 0.05 mm (0.002 inch). For the overlap joint, the distance d is assumed to be 1.32 mm (0.052 inch), creating an overlap angle of 45°. In Figure 3, the third case is included, which is identical to the butt joint except for the metal-fiber end shape. This case is called the modified-wire-end-shape joint from now on.

The hybrid composite materials considered for the models are E-glass fibers, steel fibers (i.e. metal-wire), and vinyl-ester resin. All the materials are modeled as isotropic. The elastic modulus and Poisson's ratio of E-glass fibers are 72.4 GPa and 0.22, respectively, and 207 GPa and 0.3, respectively, for steel fibers. On the other hand, the vinyl-ester resin has elastic modulus 3.5 GPa and Poisson's ratio 0.32. Both E-glass- and steel-fiber layers are assumed to have 30 percent fiber volume fractions, respectively.

Different load configurations, as shown in Figure 3, are applied to the three types of joint models. The left ends of the specimens are completely fixed while the right ends are subjected to the following loads: tension (a uniform displacement applied), shear and bending.

Previous studies showed that calculation of energy release rates was very useful for predicting the interface joint strength of composites with known critical energy release rates (Kwon *et al.*, 2008a, b; Faulkner and Kwon, 2011; Faulkner *et al.*, 2009;

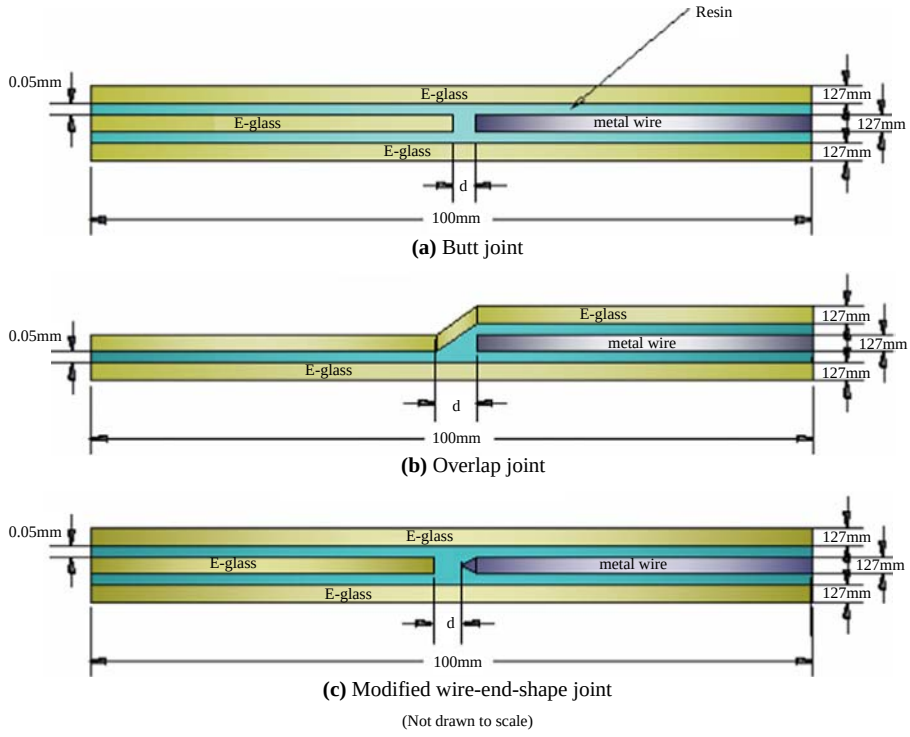

Figure 2.
Model geometries and dimensions

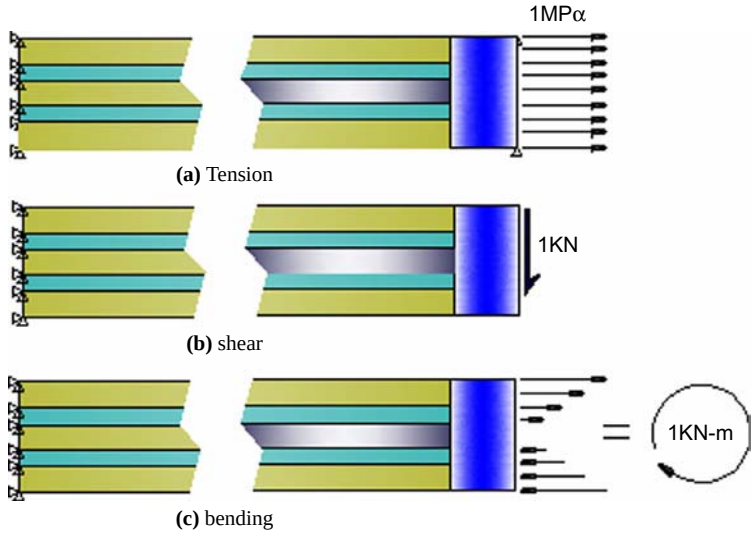

Figure 3.
Load configurations

McGuire and Harris, 1974; Harris *et al.*, 1976; Hummelgen *et al.*, 1996; Yu *et al.*, 2002; Siau *et al.*, 2005; Crane *et al.*, 2005; Kwon *et al.*, 2011; Kwon and Marron, 2009). As a result, this study also computes the energy release rates for various situations to evaluate the joint strength of the hybrid composite.

In computing energy release rates at interfaces, the critical locations where failure is most likely to occur is first determined. This is done by determining the locations that have high localized strains in the resin layers of the models without considering defects, as failure would occur through the resin layers. At the region where the resin is subjected to high strains, assumed cracks are placed at three locations: inside the resin, steel-layer/resin interface, and E-glass-layer/resin interface, because their energy releases may be different.

Previous experimental studies on interface fracture of composites showed that the crack path was always partly through the fiber/resin interface and partly through the inside of the resin layer. As a result, it was considered that the critical energy release rates were comparable between the two different crack paths since the calculated energy release rates were also very close each other. However, since the hybrid composite has two different fiber materials, two different fiber-layer/resin interface cracks as well as the cohesive crack are considered for their energy release rates. In addition, a previous experimental study gave 307 and 1,280 N/m for the critical energy release rates for the fracture modes I and II, respectively.

Initial stresses resulting from the curing process can affect the failure of composites if they are not small compared to the applied stresses. However, initial stresses may be different depending on the fiber and joint configurations as well as the curing process conditions. The failure load depends on whether the initial stresses and the applied stresses help each other or cancel each other. Since it is too complicated to consider all these variables and the objective of the study is to compare energy release rates, the initial stress state is neglected in this study.

The VCC technique requires an assumed initial flaw to be built into the finite element model. The length of this flaw is typically not known, so, often the flaw is assumed to be less than what is detectable by inspection. "Undetectable" lengths commonly vary from 0.127 mm (0.005 inch) to 0.254 mm (0.01 inch). For this research, the assumed length is set at 0.254 mm (0.01 inch) and the element crack extension Δa is set to 0.0127 mm (5 percent of crack length) for all models.

Both the standard VCC technique and a modified VCC technique (Krueger, 2002), were considered initially in this research to compute energy release rates, and their values were compared. The techniques produced results that are close each other. The difference between the two results was about 5 percent. Because this level of error is acceptable and the modified VCC technique is computationally efficient and convenient, as explained below, it is used for the rest of the study.

In the standard VCC technique, the crack in the model is physically extended, or closed, during two complete finite element analyses, as shown in Figure 4, where four-noded quadrilateral elements are used. The crack closure method is based on Irwin's crack closure integral. The method is based on the assumption that the energy released when the crack is extended by Δa from a (Figure 4(a)) to $a + \Delta a$ (Figure 4(b)) is identical to the energy required to close the crack between location ℓ and i (Figure 4(a)).

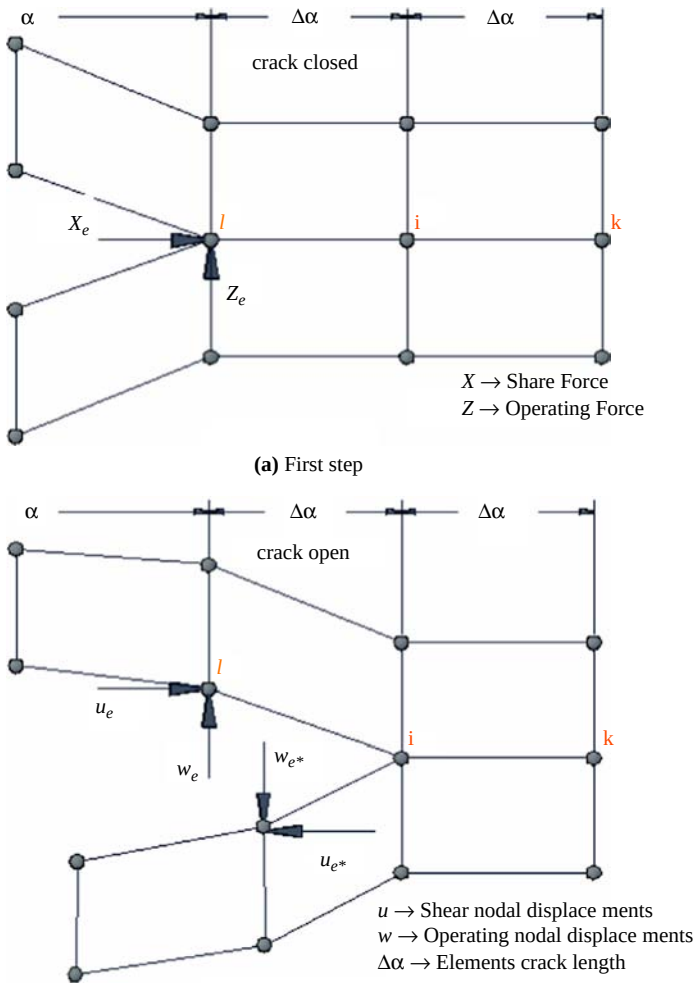

Figure 4.
Standard VCC method for four-noded element

In the standard VCC method, the energy release rates of modes I and II, G_I and G_{II}, are calculated using the following equations:

$$G_I = \frac{1}{2\Delta a} Z_\ell [w_\ell - w_{l^*}] \tag{1}$$

$$G_{II} = \frac{1}{2\Delta a} X_\ell [u_\ell - u_{\ell^*}] \tag{2}$$

As shown in Figure 4, the forces are obtained from the first finite element analysis where the crack is closed. The displacements are obtained from the second finite element analysis where the crack is extended to one full element length.

The modified VCC technique is based on the same assumptions as the standard VCC method. Additionally, however, it is assumed that a crack extension of Δa from $a + \Delta a$ (node i) to $a + 2\Delta a$ (node k) does not significantly alter the state at the crack tip (Figure 5). Therefore, the displacements behind the crack tip at node i are approximately equal to the displacements behind the original crack tip at node ℓ. Krueger (2002) outlines the details for a crack modeled with six-noded and eight-noded two-dimensional elements. Figure 5 shows the modified VCC technique using the two-dimensional six-noded elements.

In the modified VCC technique, the energy release rates of modes I and II, G_I and G_{II}, are calculated using the following equations:

$$G_I = \frac{1}{2\Delta a}[Z_i(w_\ell - w_{\ell^*}) + Z_j(w_m - w_{m^*})] \tag{3}$$

$$G_{II} = \frac{1}{2\Delta a}[X_i(u_\ell - u_{l^*}) + X_j(u_m - u_{m^*})] \tag{4}$$

In addition to the forces X_i and Z_i at the crack tip, the forces X_j and Z_j at the mid-side node in front of the crack are required. Furthermore, in addition to the relative sliding and opening at nodal points ℓ and ℓ^*, the relative displacements at nodal points m and m^* are required. Because the modified VCC technique requires only one analysis, it is more efficient and convenient.

3. Results and discussion

1. Tensile load

In order to determine the critical locations of joint interfaces for potential failure, effective strains are computed, without considering any crack under tension. The regions of high strain for the butt joint are located around the left-edge corners of the metal-wire. For the overlap join, three critical crack locations were considered since the resulting plot shows three regions of high strains. In the case of the modified-wire-end-shape joint, the regions of high strain are located at the apex and corners of the middle-layer tip. Virtual cracks are placed at the critical locations of each joint, as shown in Figures 6 through 8.

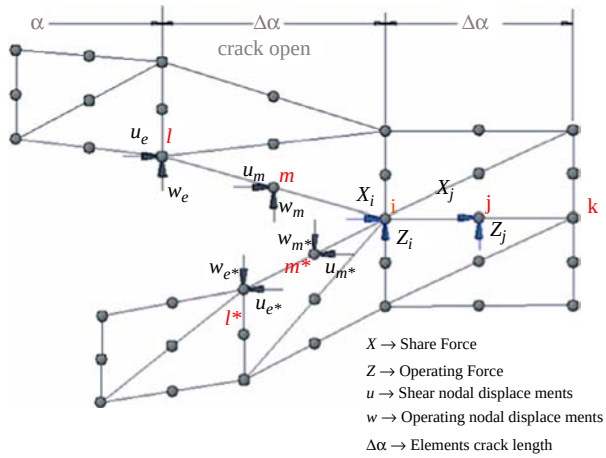

Figure 5.
Modified VCC method for six-noded element

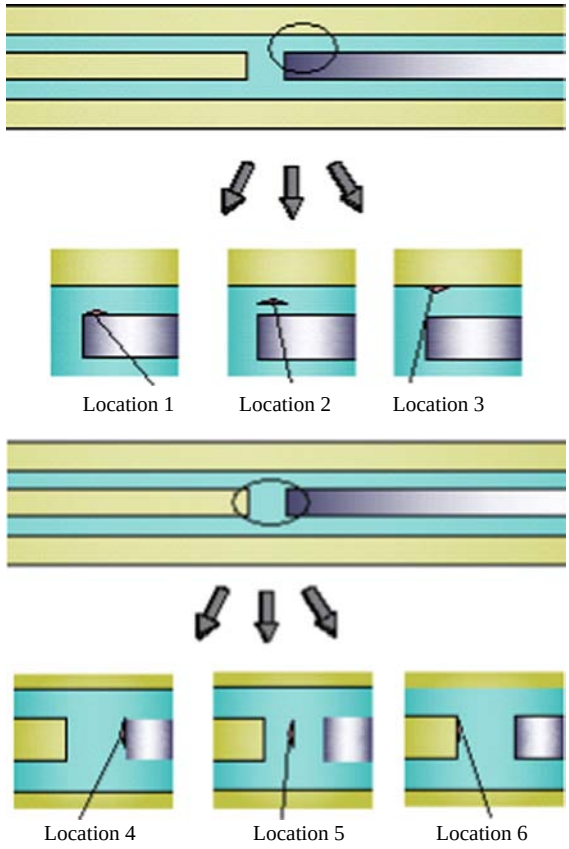

Figure 6.
Virtual crack embedded in critical locations of butt joint

Because of symmetry of the butt joint and modified-wire-end-shape joint about their horizontal centerline, horizontal cracks are considered only at the upper side.

For butt joints, the outer fiber layers carry most of the load at the joint due to the discontinuity of the middle fiber layers. Because of the discontinuity, the load transfer from the left middle fiber layer to the right middle fiber layer occurs though shear stress between the middle fiber layers and the surrounding resin layer. In addition, the resin between the two discontinuous fiber layers is under tensile stress. Thus, the onset of crack growth in resin may occur due to the interlaminar shear stress between the middle and outer fiber layers and the tensile stress between the two middle fiber layers' tips. As a result, virtual cracks are introduced separately to the resin between the middle and outer fiber layers, and between the two middle fiber layers' tips, as shown in Figures 6 through 8, to determine their energy release rates. Horizontal cracks are considered between the middle and outer fiber layers while vertical cracks are included between the middle fiber layers' tips, because the second mode of fracture is dominant for the former location and the first mode is critical for the latter locations.

Even though a crack may have various orientations at each critical location, the major orientation in compliance with the load-carrying direction is considered.

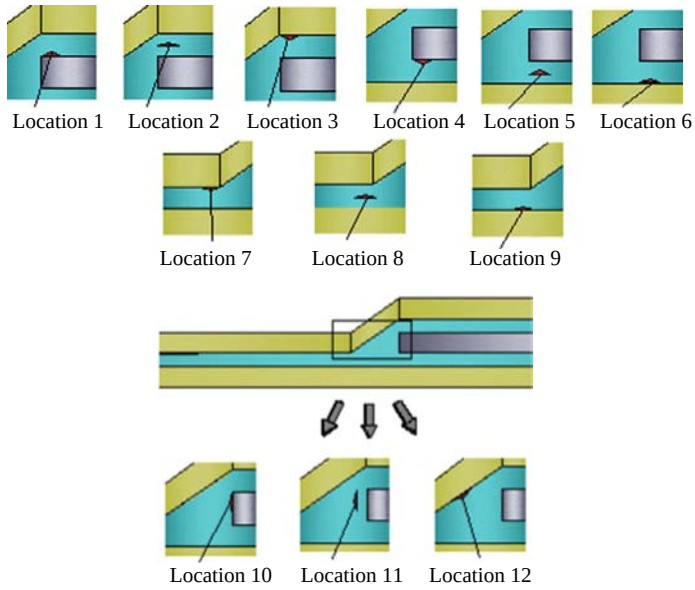

Figure 7.
Virtual cracks embedded in critical locations of overlap joint

Otherwise, it would require virtually unlimited numbers of analyses to find the most critical crack orientation. Besides, because the present study is to compare the effectiveness of different joint configurations rather than prediction of failure strength, it is decided that the detailed crack orientation analyses would not be necessary.

For the butt joint, locations nos 1 through 3 in Figure 9 show that the forces acting on the crack tips are closing in nature. This means that the mode I energy release rate component is non-existent and the energy release rate is purely mode II for resin cracks located between the fiber layers. The energy release rate results show that the crack inside the resin (location no. 2 in Figure 9) has the greatest energy release rate for the butt joint even though the difference is very small. In all energy release rate plots, unless mentioned otherwise, they were normalized in terms of a unit value of applied force or moment.

In locations nos 4 through 6 in Figure 10, it was observed that the forces acting on the crack are tensile in nature and the shear forces are negligible. Thus, the mode I energy release rate component characterizes the failure of cracks existing between the middle fiber layers' tips. Figure 10 shows that location no. 5, which is the crack located inside the resin, is the most critical case even though the difference is small. Both results from Figures 9 and 10 show that the energy release rate is more or less the same either inside the resin or at the fiber-layer/resin interfaces. These results as well as other previous experimental observation suggest that it is not necessary to distinguish cracks based on whether they are located between fiber-layer/resin interfaces or inside the resin material for the butt joint.

Furthermore, another comparison is made when the metal-fiber layer is replaced by the E-glass fiber layer in the butted joint in Figures 9 and 10, i.e. a uniform E-glass composite joint. This comparison is to exhibit the difference of energy release rates between the hybrid joint (E-glass to steel fibers) and the uniform joint (E-glass to E-glass fibers). Figures 11 and 12 clearly show the difference. The hybrid joint has

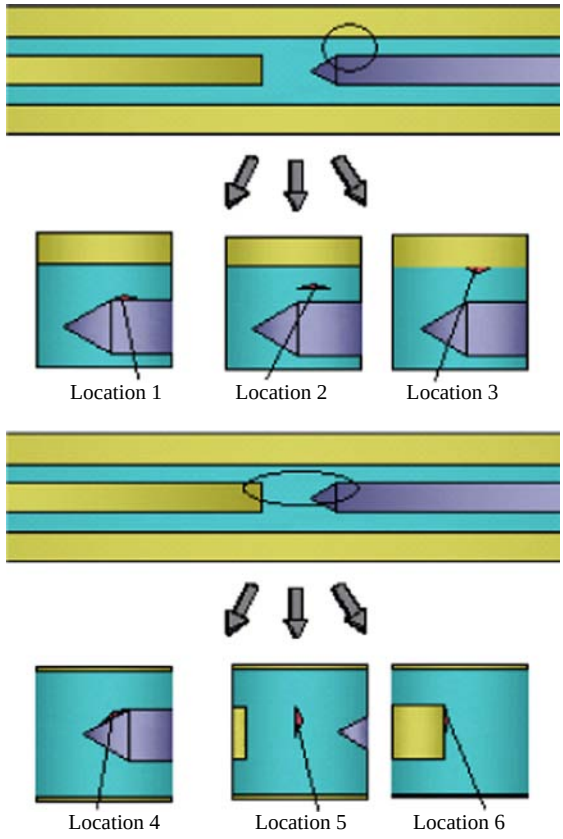

Figure 8.
Virtual cracks embedded in critical locations of modified-wire-end-shape joint

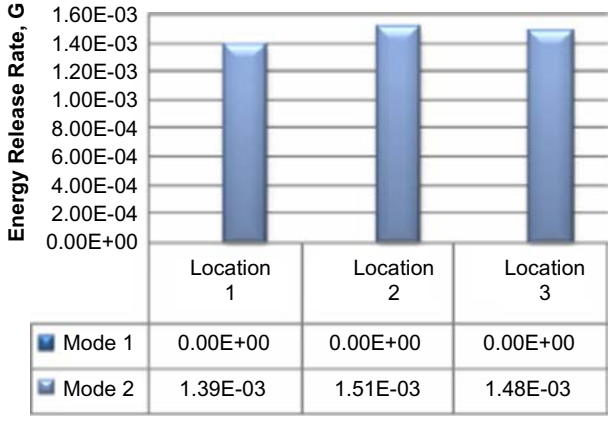

Note: See Figure 6 for crack locations

Figure 9.
Energy release rate of resin cracks between middle and outer fiber layers of butt joint

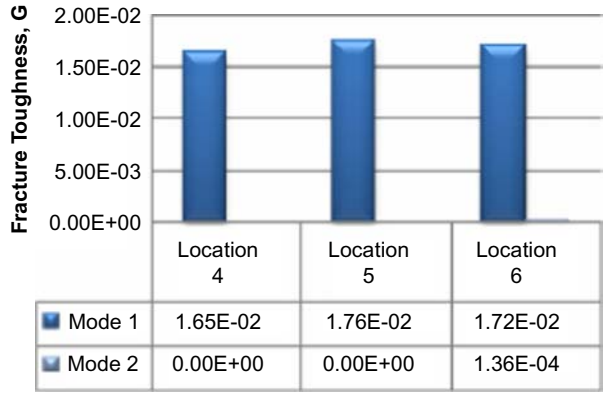

Note: See Figure 6 for crack locations

Figure 10.
Energy release rate of resin cracks between middle fiber layers' tips of butt joint

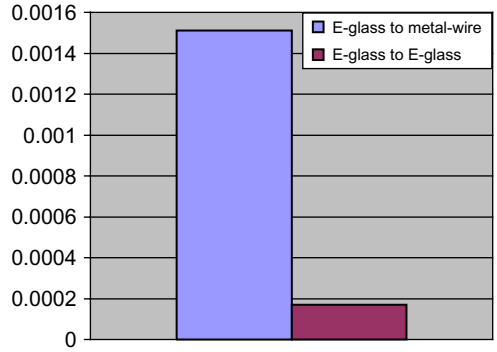

Figure 11.
Comparison of energy release rates of mode II between hybrid and uniform butt joints for crack between outer and middle fiber layers

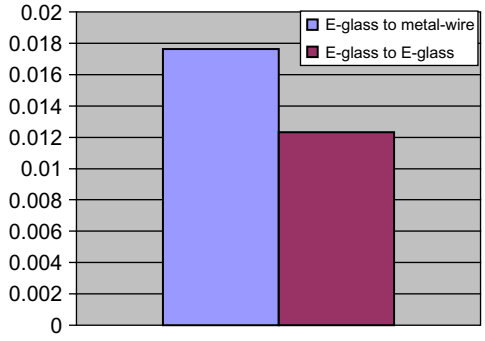

Figure 12.
Comparison of energy release rates of mode I between hybrid and uniform butt joints for crack between two middle layers' ends

higher energy release rates for both modes I and II. This result indicates that the hybrid joint is more susceptible to interface failure assuming the fracture toughness is not much different between the hybrid and uniform joint interfaces. This is quite true, as we observed in a previous testing that the interface fracture toughness was rather independent of the fiber materials, either E-glass or carbon fibers, as long as the same resin was used in the composites (Kwon *et al.*, 2008a).

The next result is for the overlap joint. In locations nos 1 through 9 in Figure 13, it was observed that the interface forces acting on the crack were shear only except for location no. 9. This means that all crack locations have only mode II energy release rate while location no. 9 has mixed modes of energy release rate. However, the mode I component at location no. 9 is much smaller than the mode II component. Among these locations, locations nos 7-9 in Figure 13 have the largest energy release rates.

In locations nos 10 and 11 in Figure 14, the mode I component is generally the more significant component of failure for the cracks located between the fiber layer tips,

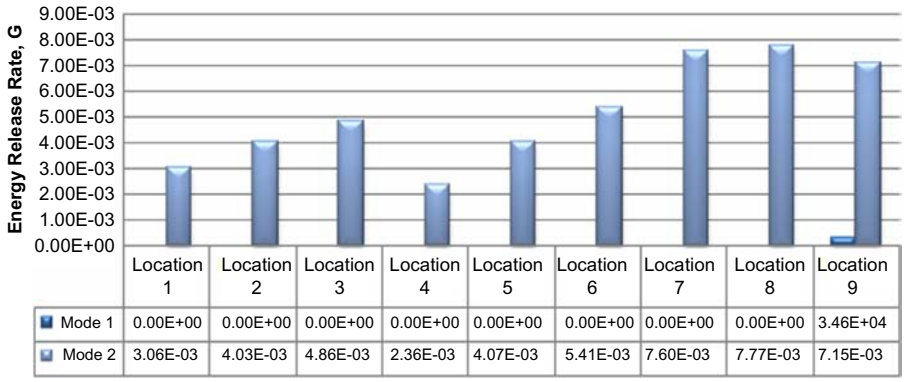

	Location 1	Location 2	Location 3	Location 4	Location 5	Location 6	Location 7	Location 8	Location 9
Mode 1	0.00E+00	0.00E+00	0.00E+00	0.00E+00	0.00E+00	0.00E+00	0.00E+00	0.00E+00	3.46E+04
Mode 2	3.06E-03	4.03E-03	4.86E-03	2.36E-03	4.07E-03	5.41E-03	7.60E-03	7.77E-03	7.15E-03

Note: See Figure 7 for crack locations

Figure 13.
Energy release rate of resin cracks between the middle and outer fiber layers of overlap joint

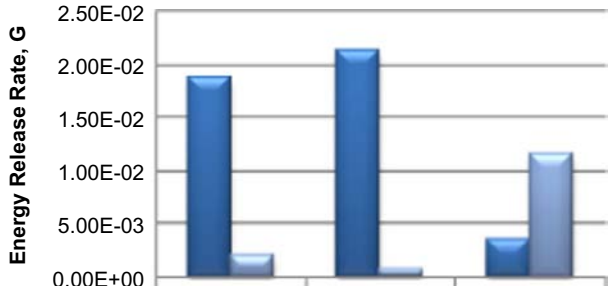

	Location 10	Location 11	Location 12
Mode 1	1.88E-02	2.13E-02	3.56E-03
Mode 2	2.07E-03	6.74E-04	1.15E-02

Note: See Figure 7 for crack locations

Figure 14.
Energy release rate of resin cracks between middle fiber layers' tips

as expected. However, the results for the crack in location no. 12 show that the mode II component is greater than the mode I component. Since mode I failure usually has a lower threshold value than mode II, modes I and II are equally critical for location no. 12. Comparing the three locations, location no. 11, i.e. a vertical crack inside the resin between two middle fiber layers' tips, is considered the most critical case.

As far as the modified-wire-end-shape butt joint is concerned, similar to the previous butt joint, the mode II component characterizes the delamination failure for resin cracks located between the outer and middle fiber layers as shown in locations nos 1 through 3 in Figure 15. The energy release rate results show that the crack along the E-glass interface (location no. 3 in Figure 15) is the most critical case. Comparing the results in Figures 9 and 15 shows that the critical location between the outer and middle fiber layers has shifted from inside the resin to the interface between the resin and the outer E-glass-layer as the wire-end shape is modified.

In locations nos 4 through 6 in Figure 16, the forces acting on the crack tips are dominantly tensile in nature, as expected, even though there are small shear forces there. Thus, the mode I energy release rate component characterizes the potential failure of cracks existing between the middle fiber layers' tips. Location no. 6, which is the crack located along the E-glass-layer interface with resin, is the most critical case.

When all three joint configurations are compared, the overlap joint has the highest energy release rate results for cracks in all considered locations. For cracks between the outer and middle fiber layers, the butt joint has lower energy release rates than the modified-wire-end-shape joint. However, for cracks between the two middle fiber layers' tips, the modified-wire-end-shape joint has lower energy release rates. In the crack locations investigated, the most critical cases for the butt joint and overlap joint are the cracks inside the resin. For the modified-wire-end-shape joint, cracks along the E-glass-layer/resin interface are the most critical cases.

Based on these results, in cases where failure is expected between the outer and middle fiber layers, the butt joint is the best to be considered. If failure is to occur in between the middle layers' tips, the modified-wire-end-shape joint is proposed. the overlap joint design can be considered under small tension loading.

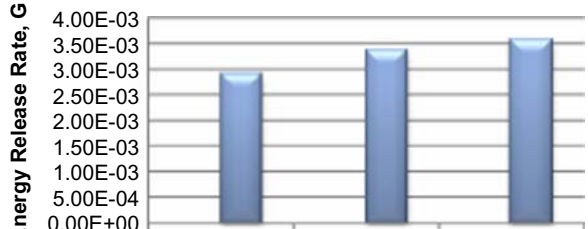

	Location 1	Location 2	Location 3
Mode 1	0.00E+00	0.00E+00	0.00E+00
Mode 2	2.91E-03	3.37E-03	3.58E-03

Note: See Figure 8 for crack locations

Figure 15.
Energy release rate of resin cracks between outer and middle fiber layers of modified-wire-end-shape joint

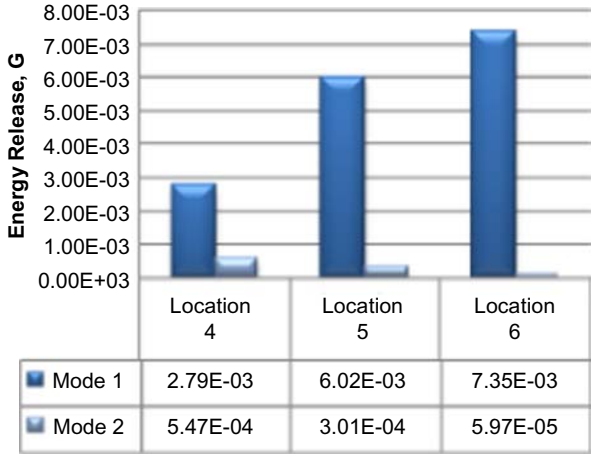

Note: See Figure 8 for crack locations

Figure 16.
Energy release rate of resin cracks between two middle fiber layers' tips of modified-wire-end-shape joint

Further investigation is made to determine the influence of the resin area between the middle fiber layers' tips and the wire-end geometry on the butt and modified-wire-end-shape joints. This is done by applying a tensile load to the models and extending the gap *d* between the middle layers, as shown in Figure 17, to the point where the middle fiber layers' tips have no significant interaction. The numerical results confirm that the wire-tip geometry has a minimal effect on the energy release rate of the crack in a very wide gap. As the gap *d* changes incrementally, the shear stress in the resin between the two middle layers near their tips is compared. The results show that as the resin area in between the layers' tips is increased, the shear stresses between the outer and middle fiber layers near the fiber discontinuity also increase. This means that with a greater resin area between the middle fiber layers' tips, the resin deforms more freely, thereby shifting some of the load to the resin between the outer and middle fiber layers near the fiber discontinuity, carried in the form of shear stress.

Figure 17 shows the load transfer between the middle fiber layers' tips represented by the field lines for the same gap *d*. In the case of the butt joint, which has a very small area filled by the resin, the force fields are more concentrated at the tip edges, thereby having less influence on the crack locations nos 1 through 3 in Figure 6, while having greater

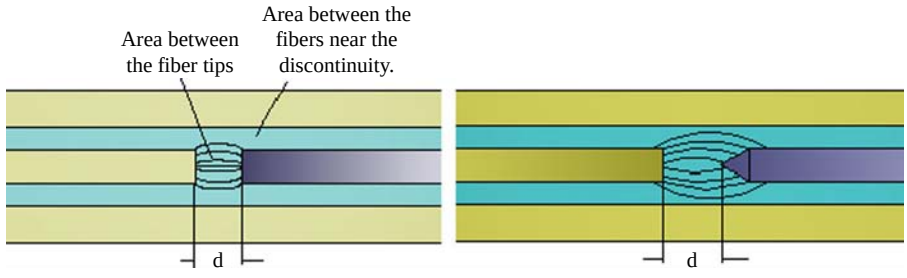

(a) Butt joint.

(b) Modified wire end shape joint

Figure 17.
Middle fiber interaction of the butt joint and modified-wire-end-shape joint

influence on the cracks in locations 4 through 6 in Figure 6. In the case of the modified-wire-end-shape joint, which has a larger resin area between the tips, the force fields are not as concentrated as those for the butt joint. This allows the resin between the middle layers' tips to deform more freely, which influences the cracks in locations nos 1 through 3 in Figure 7 and has less influence on the crack locations nos 4 through 6 in Figure 7 by shifting some of the load to the resin between the outer and middle layers near the fiber discontinuity. As a result, the butt joint has a higher energy release rate between the middle layers' tips than the modified-wire-end joints, while the latter has a greater energy release rate between the middle and outer fiber layers than the former.

For the overlap joint, varying the overlap angle changes the area filled by the resin between the inclined edge and the middle fiber layer tip, as shown in Figure 18. This influences the energy release rate of the cracks in the same way as described above.

2. Shear load

The critical locations under shear loading are the same as those under tensile loading. Therefore, virtual cracks are introduced into the same locations as shown in Figures 6 through 8. Because shear loading produces an asymmetric solution, it is necessary to investigate virtual cracks located between the top and middle fiber layers as well as the bottom and middle fiber layers. Instead, we consider cracks only between the top and middle fiber layers while the shear loading is applied in either the upward or downward direction, respectively. Shear loading in the upward and downward directions results in different solutions at the same crack location with either crack opening or crack closure. For the latter case, mode I does not contribute to fracture.

In locations nos 1 through 3 in Figure 19 of the butt joint, it is observed that the forces acting on the crack tip are closing in nature with the shear loading in the downward direction. The mode I energy release rate component is non-existent and the energy release rate is purely mode II for cracks located between the top and middle fiber layers. The energy release rate results show that the crack inside the resin (location no. 2 in Figure 19) is the most critical case.

With the shear load reversed (now in the upward direction) Figure 20 shows the existence of modes I and II. This means that the forces acting on the crack are opening in nature when the upper part of the butt joint is under compression. Results yield the same mode II values, except that in this case mode I components are present. Comparing Figures 19 and 20 states that the crack on the compression side of the butt joint is more critical when the shear loading is applied.

Figure 21 shows the results for the crack locations nos 4-6 for shear loading in the downward direction. The energy release rate of mode I is almost the same for the three

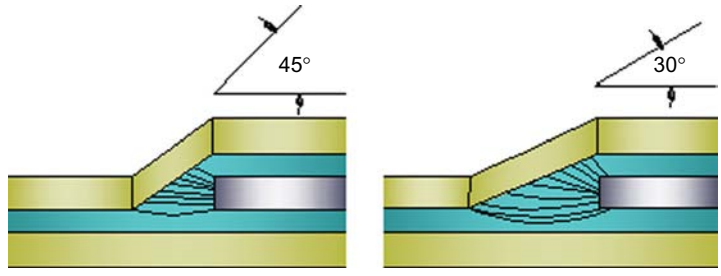

Figure 18.
Metal wire tip and inclined edge interaction of the overlap joint

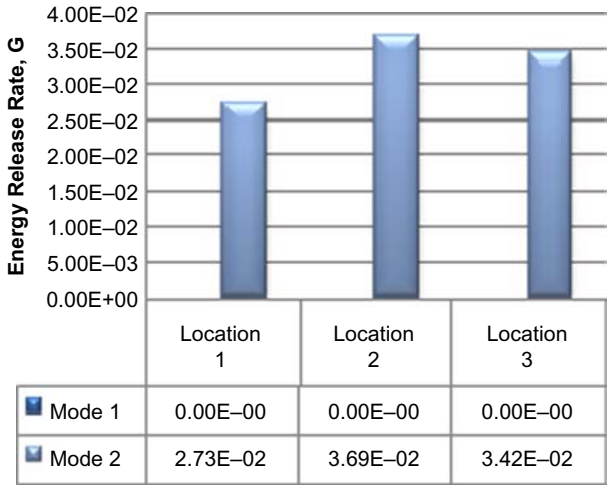

Figure 19.
Energy release rate of resin cracks between the outer and middle fiber layers of butt joint with shear loading in downward direction

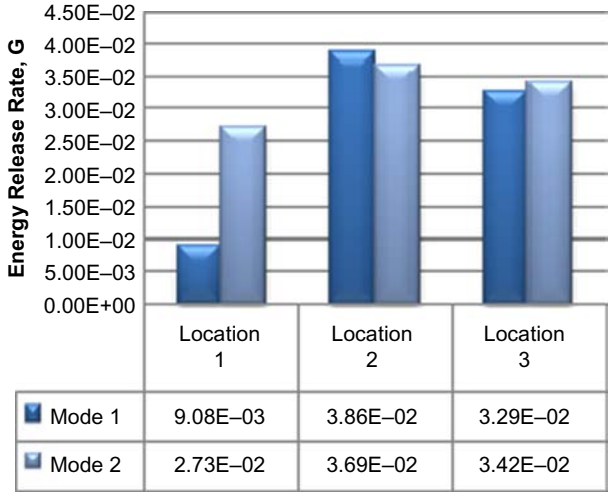

Figure 20.
Energy release rate of resin cracks between top and middle fiber layers of butt joint with shear loading in upward direction

crack locations. Shear loading in the upper direction reveals almost the same energy release rates because the cracks are located at the horizontal centerline of the butt joint.

Figure 22 is for the overlap joint with the shear load in the downward direction, and it shows that location no. 8 is the most critical case. On the other hand, Figure 23, with the shear load in the upward direction, shows that locations nos 2 and 5 are the most critical cases. Depending on the shear loading direction, failure is expected to initiate at different locations. Depending on the critical energy release rates of modes I and II as well as the mixed fracture criterion, the shear loading in one direction will be more critical than in the other direction. For example, if the mode I fracture has a much lower critical energy release rate than mode II, location no. 2 in Figure 23 will be the

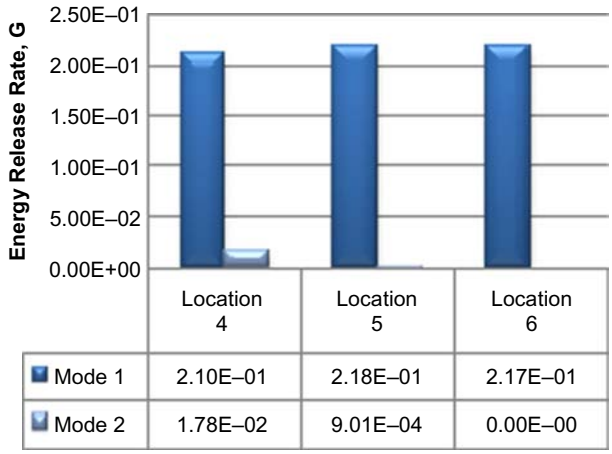

Figure 21.
Butt joint: energy release rate of resin cracks between the layer tips with shear loading in downward direction

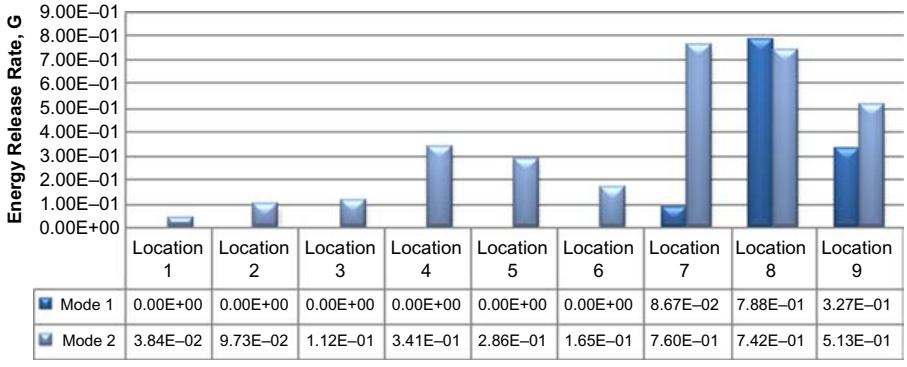

Figure 22.
Overlap joint: energy release rate of resin cracks between top and middle fiber layers of overlap joint with shear loading in downward direction

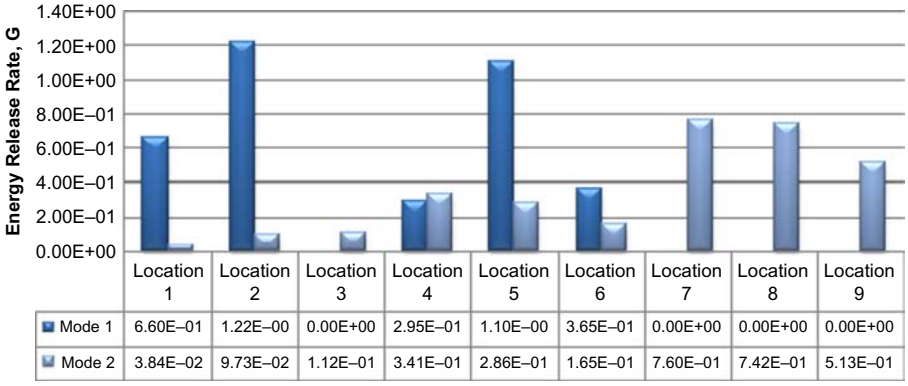

Figure 23.
Overlap joint: energy release rate of resin cracks between top and middle fiber layers of overlap joint with shear loading in upward direction

most critical. This means the shear loading in the upward direction will cause the joint failure at a lower load.

Figure 24 shows the results for shear loading in the downward direction. Shear loading in the upper direction yields almost the same mode II results except that the mode I components are non-existent. Results show that location no. 11 is expected to be the most critical case.

As far as the modified-wire-end-shape butt joint is concerned, the energy release rates are very similar to those of the standard butt joint when the shear loading is applied in the downward direction. The magnitude is about twice as high for the modified-wire-end-shape joint. However, when the shear loading is reversed, which is the more critical case, the distribution of modes I and II as well as their magnitudes are quite different from those for the standard butt joint. As Figure 25 is compared to Figure 20, it is found that the modified end-shape has much greater mode II energy release rate than mode I, especially for location no. 3.

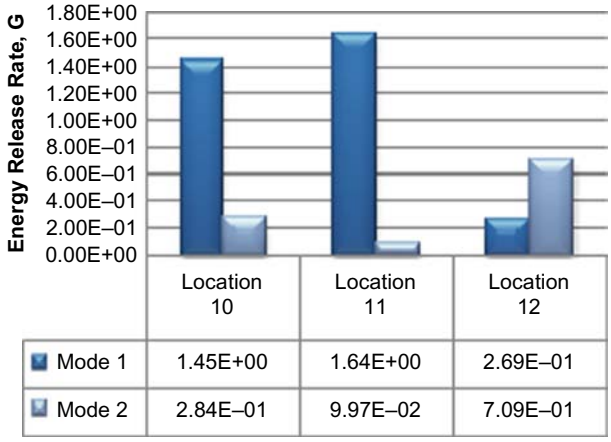

Figure 24.
Energy release rate of vertical resin cracks of overlap joint with shear loading in upward direction

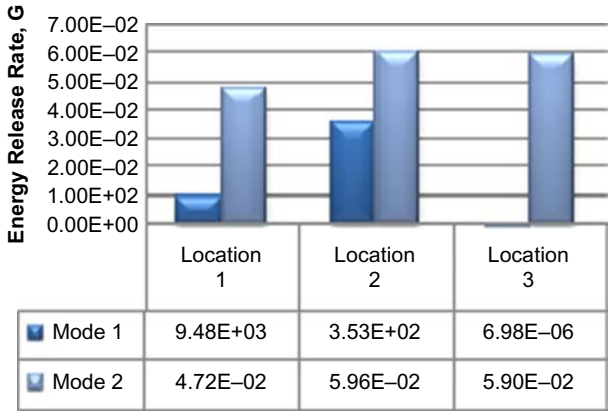

Note: Shear loading in the upward direction

Figure 25.
Modified-wire-end-shape joint: energy release rate of resin cracks between the fibers

In summary, for the shear loading, there is a mixed mode of fracture depending on the loading direction. However, like with the tensile loading, the overlap joint has the highest energy release rates than the other joints. For cracks between the top and middle fiber layers, the butt joint gives lower energy release rates than the modified-end-shape joint. For the cracks between the middle fiber layers' tips, the modified-end-shape joint gives lower results. Generally, the most critical case for each joint is the crack inside the resin rather than at the resin/fiber-layer interface.

3. Bending load

Both clockwise (CW) and counter-clockwise (CCW) bending moments are applied, respectively, to the joints for cracks between the top and middle fiber layers, as explained for the shear loading. The critical locations under the bending loads are the same as those in the previous study.

The CCW bending was considered for cracks in locations nos 1-3 of the butt joint since the mode I component for CW loading is non-existent for these locations. Figure 26 shows location no. 2, which is the crack inside the resin, to be the most critical case. In Figure 27, although there is no significant difference among the energy release rates of locations nos 4 through 6, location no. 4 has a small fraction of the mode II component.

For the overlap joint under CW bending loading, Figure 28 shows that location no. 8 is the most critical, while Figure 29 with CCW bending shows that location no. 5 is the most critical case. Both critical cracks lie inside the resin material. The actual failure will depend on the criticality of each fracture mode and their interaction as a mixed mode. Figure 30 shows the results for cracks between the middle layers' tips under CW bending. Results show that location no. 11 is the most critical case.

For the modified-end-shape joint under CW bending, mode I and II components are present as shown in Figure 31, while in CCW bending, mode I components are non-existent due to the closing nature of the forces acting on the crack tips. The energy release rate is largest at location no. 2 in Figure 31. The most critical location between the middle fiber layers' tips is either location nos 5 or 6 as shown in Figure 32, depending on the critical value of each mode at the respective locations.

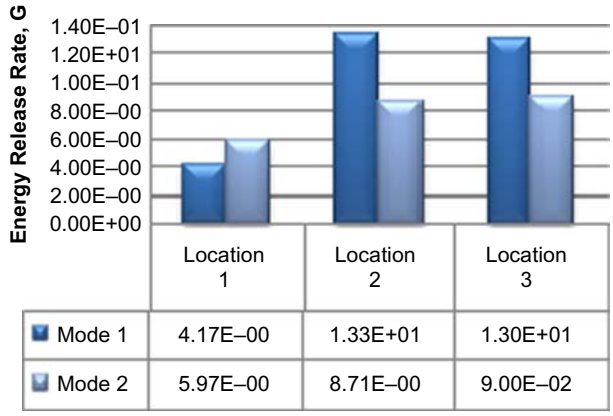

Figure 26.
Energy release rate of resin cracks between top and middle fiber layers of butt joint under CCW bending

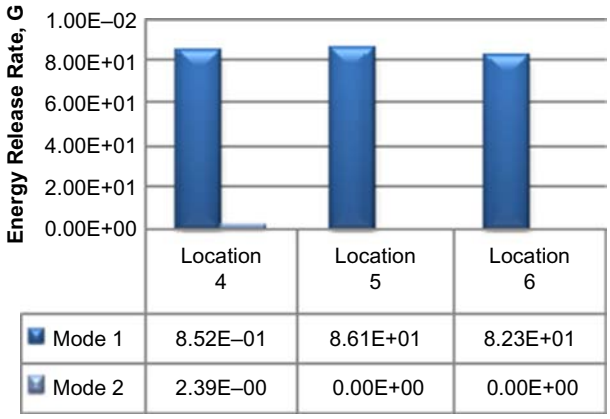

Figure 27.
Energy release rate of resin cracks between middle fiber layers' tips under CW bending

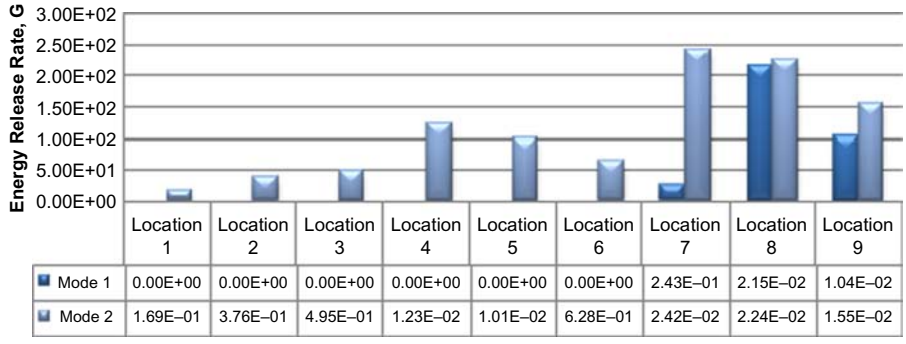

Figure 28.
Energy release rate of resin cracks between top and middle fiber layers of overlap joint with CC bending

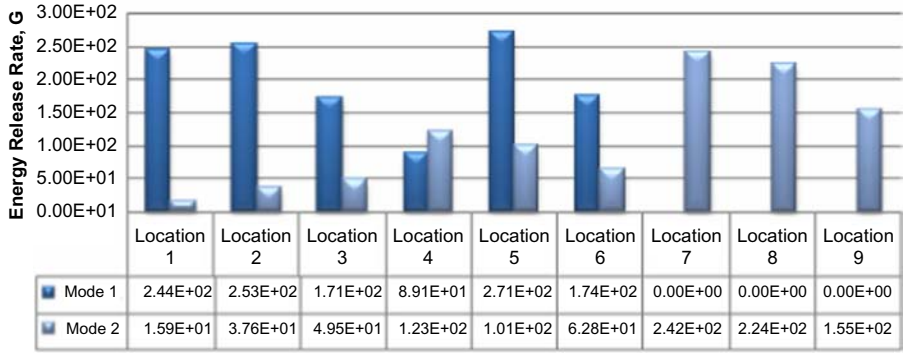

Figure 29.
Energy release rate of resin cracks between top and middle fiber layers of overlap joint with CCW bending

4. Conclusions

The joint interface of a hybrid composite consisting of E-glass- and steel-fiber layers is much more susceptible to failure than the joint interface of the layers made of the same fiber materials. Therefore, it is critical to evaluate the joint interface strength of a hybrid composite. In all cases that were investigated, the butt joint is considered as the best joint if potential cracks are located between the outer and middle fiber layers while

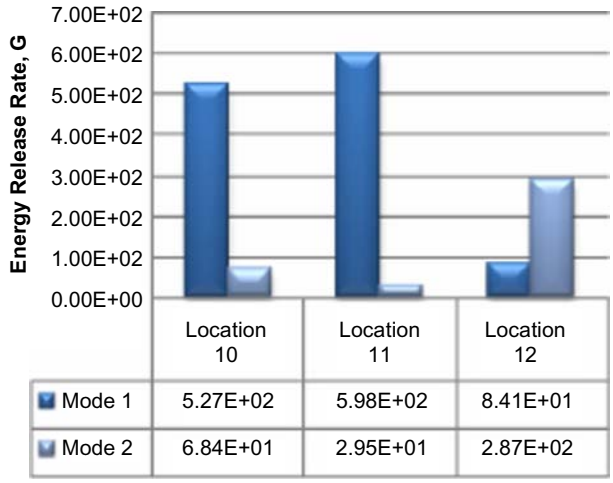

Figure 30.
Overlap joint: energy release rate of resin cracks between the fibers

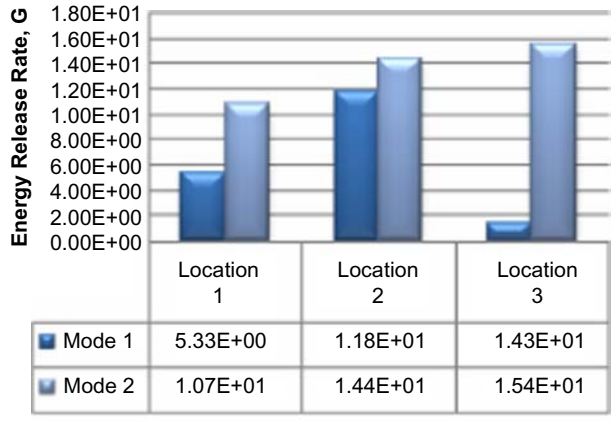

Figure 31.
Energy release rate of resin cracks between top and middle fiber layers for modified wire-end-shape joint under CW bending

the modified-wire-end-shape is the joint to be considered if potential cracks are present between the middle fiber layers' tips. The overlap joint is expected to carry much less loading because of higher energy release rates of interface cracks. This statement is quite general regardless of the loading types and their directions. When comparing different crack locations such as inside the resin or at the fiber-layer/resin interfaces, inside-the-resin cracks generally show higher energy release rates even though there are some exceptions depending on the loading types and directions as well as the joint configurations. This means if the critical energy release rate is the same or at least very close between the inside of the resin layer or at the fiber-layer/resin interfaces as shown in some previous experimental studies, failure will initiate inside the resin material in most cases. This study will provide useful information in designing a hybrid composite to join metallic and polymer composite structures.

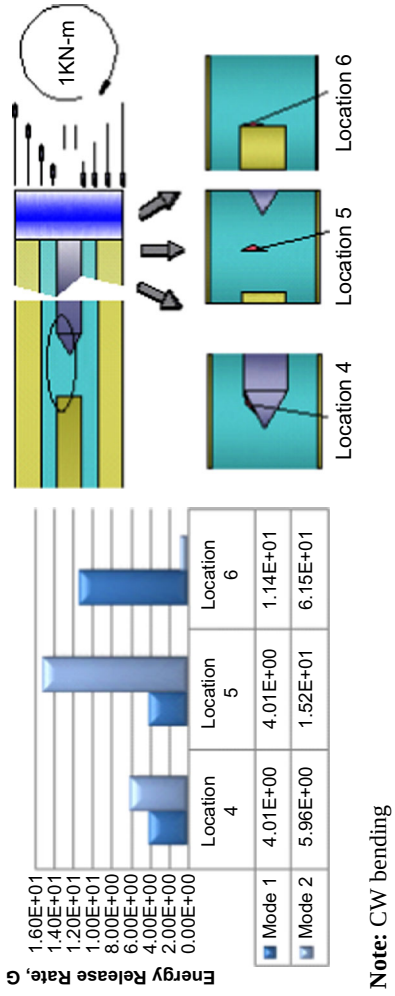

Note: CW bending

Figure 32.
Modified-wire-end-shape joint: energy release rate of resin cracks between the fibers

References

Baker, A.A., Chester, R.J., Hugo, G.R. and Radtke, T.C. (1999), "Scarf repairs to highly strained graphite/epoxy structure", *International Journal of Adhesion and Adhesives*, Vol. 19, pp. 161-71.

Caccese, V., Kabche, J.-P. and Berube, K.A. (2007), "Analysis of a hybrid composite/metal bolted connection subjected to flexural loading", *Composite Structures*, Vol. 81 No. 3, pp. 450-62.

Caccese, V., Mewer, R. and Vel, S.S. (2004), "Detection of bolt load loss in hybrid composite/metal bolted connections", *Engineering Structures*, Vol. 26, pp. 895-906.

Cheuk, P.T., Tong, L., Wang, C.H., Baker, A. and Chakley, P. (2002), "Fatigue crack growth in adhesively bonded composite-metal double-lap joints", *Composite Structures*, Vol. 57 Nos 1-4, pp. 109-15.

Crane, M., Robbins, T. and Graham, S. (2005), "Influence of joint geometry on tensile strength of a co-cured symmetric stepped-lap joint", paper presented at SAMPE-2005 Conference, Long Beach, CA, May 1-5.

Erdogan, F. and Ratwani, M. (1971), "Stress distribution in bonded joints", *Journal of Composite Materials*, Vol. 5, pp. 378-93.

Faulkner, S.D. and Kwon, Y.W. (2011), "Fracture toughness of composite joints with carbon nanotube reinforcement", *ASME Journal of Pressure Vessel Technology*, Vol. 133 (in press).

Faulkner, S.D., Kwon, Y.W., Bartlett, S. and Rasmussen, E.A. (2009), "Study of composite joint strength with carbon nanotube reinforcement", *Journal of Materials Science*, Vol. 44 No. 11, pp. 2858-64.

Ganesh, V.K. and Choo, T.S. (2002), "Modulus graded composite adherends for single-lap bonded joints", *Journal of Composite Materials*, Vol. 36, pp. 1757-67.

Gunnion, A.J. and Herszberg, I. (2006), "Parametric study of scarf joints in composite structures", *Composite Structures*, Vol. 75, pp. 364-76.

Harris, B., Ankara, A.O. and McGuire, M.A. (1976), "Fatigue crack propagation in metal-matrix/metal-fiber composites", *J. Phys. D: Appl. Phys.*, Vol. 9, pp. 365-72.

Hart-Smith, L.J. (1973), "Adhesively-bonded scarf and stepped-lap joints", NASA Technical Report CR 112237.

Hummelgen, I.A., Roman, L.S., Nart, F.C., Peres, L.O. and de Sa, E.L. (1996), "Polymer and polymer/metal interface characterization via Fowler-Nodheim tunneling measurements", *Appl. Phys. Lett.*, Vol. 68 No. 22, pp. 3194-6.

Ishii, K., Imanaka, M., Nakayama, H. and Kodama, H. (1998), "Fatigue failure criterion of adhesively bonded CFRP/metal joints under multiaxial stress conditions", *Composites Part A: Applied Science and Manufacturing*, Vol. 29 No. 4, pp. 415-22.

Krueger, R. (2002), "The virtual crack closure technique: history, approach and applications", NASA/CR-211628.

Kwon, Y.W. and Marron, A. (2009), "Scarf joints of composite materials: testing and analysis", *Applied Composite Materials*, Vol. 16 No. 6, pp. 365-78.

Kwon, Y.W., Greene, T.R. and Bartlett, S. (2008a), "Development of multiscale modeling techniques for composite scarf joints", paper presented at The Sixth International Conference on Engineering Computer Technology, Athens, Greece, September.

Kwon, Y.W., Slaff, R., Bartlett, S. and Greene, T. (2008b), "Enhancement of composite scarf joint interface strength through carbon nanotube reinforcement", *Journal of Materials Science*, Vol. 43, pp. 6695-703.

Kwon, Y.W., Schultz, W.A., Loup, D.C. and Rasmussen, E.A. (2011), "Experimental study of mode II fracture of hybrid composite and metal-wire joints", *ASME Journal of Pressure Vessel Technology*, Vol. 133 (in press).

Loftus, D., Found, M.S. and Yates, J.R. (2002), "The performance of aluminum to carbon fibre composite bonded joints in motorsport applications", *Sports Engineering*, Vol. 2 No. 4, pp. 235-43.

Lubkin, J.L. (1957), "A theory of adhesive scarf joints", *Journal of Applied Mechanics*, Vol. 24, July, pp. 255-60.

McGuire, M.A. and Harris, B. (1974), "Crack propagation in metal-matrix/metal-fiber composites: I. Strength and toughness", *J. Phys. D: Appl. Phys.*, Vol. 7, pp. 1788-802.

Pipes, R.B., Adkins, D.W. and Deaton, J. (1982), "Strength and repair of bonded scarf joints for repair of composite materials", MSG 1304, NASA Langley Research Center, Hampton, VA.

Siau, S., Vervaet, A., Vaeck, L.V., Schacht, E., Demeter, U. and Van Calster, A. (2005), "Adhesion strength of the epoxy polymer/copper interface for use in microelectronics", *Journal of Electrochemical Society*, Vol. 152 No. 6, pp. C442-55.

Sihn, S., Myano, Y., Najada, M. and Tsai, S.W. (2003), "Time- and temperature-dependent failures of a metal-to-composites bonded joint with PMMA adhesive material", *Journal of Composite Materials*, Vol. 37 No. 1, pp. 35-54.

Yu, J., Song, J.Y. and Park, I.S. (2002), "Analyses of the practical adhesion strengths of metal/polymer interfaces in electronic packaging", *Journal of Electronic Materials*, Vol. 21 No. 12, pp. 1347-52.